NREL
Transforming ENERGY

EERA DeepWind 2025 Conference
January 15-17, 2025, Trondheim, Norway

OpenFAST Simulation of Floating Offshore Wind Turbines with Large Heading Change

Lu Wang[1], **Jason Jonkman**[1],
[1] National Renewable Energy Laboratory (NREL)

Photo by Dennis Schroeder, NREL 55200

Introduction

Before OpenFAST v4, substructure rotation was assumed to be small (pitch-roll-yaw sequence doesn't matter).

This is adequate for most design load cases (DLCs) with some exceptions where large yaw/heading change is expected:

- Transient drift after mooring-line failure (DLC 9.1 and DLC 10.1 of IEC 61400-3-2 [1])
- Weathervaning of FOWT designs with single-point mooring, e.g., T-Omega Wind [2]
- Designs with FOWT atop one of the offset columns instead of a central column

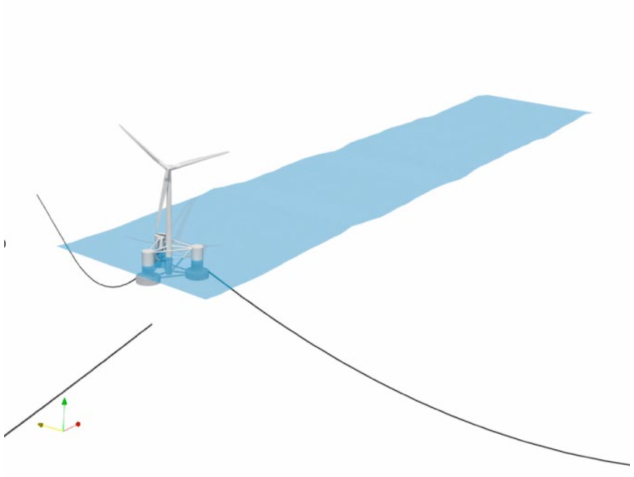

Transient drift after mooring-line failure

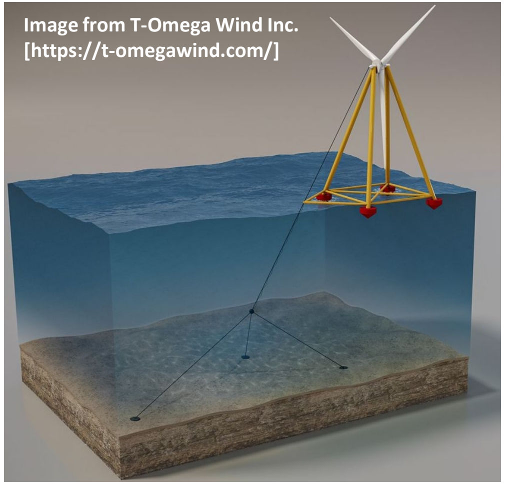

Weathervaning FOWT designs [2]

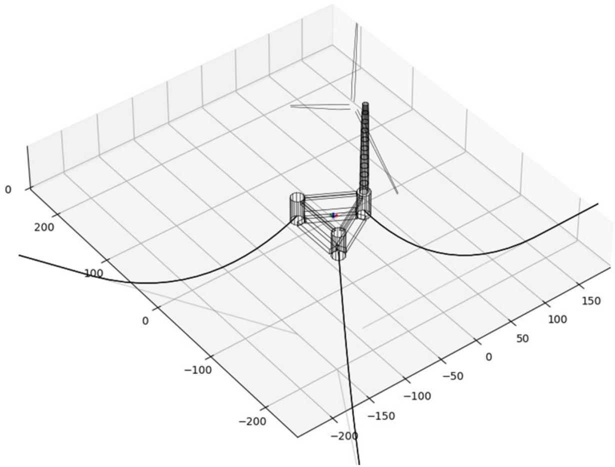

FOWT on offset column

[1] International Electrotechnical Commission, Wind energy generate systems – Part 3-2: Design requirements for floating offshore wind turbines, IEC TS 61400-3-2, International Electrotechnical Commission, Geneva, Switzerland.

[2] Wang, L., Jonkman, J., Papadopoulos, J., and Myers, A.T., (2023). OpenFAST modeling of the T-Omega wind floating offshore wind turbine system, in Proc. ASME 5th Int. Offshore Wind Tech. Conf., Exeter, UK. doi:10.1115/IOWTC2023-119410.

- Substructure (platform) rotation assumed to be small/moderate in previous versions of OpenFAST [3]:

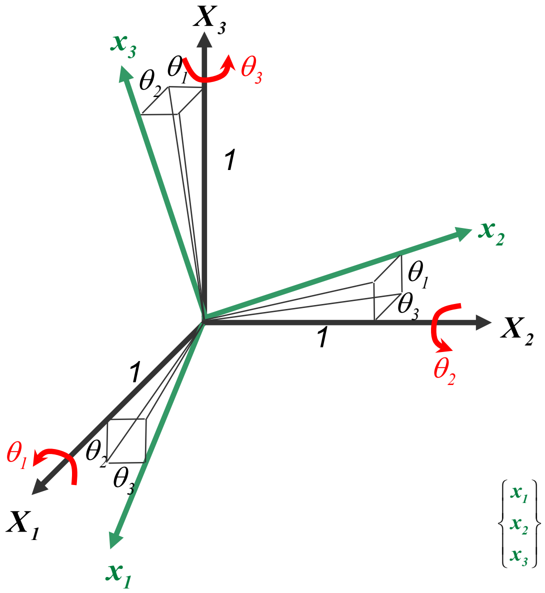

$$\begin{Bmatrix} x_1 \\ x_2 \\ x_3 \end{Bmatrix} \approx \overbrace{\begin{bmatrix} 1 & \theta_3 & -\theta_2 \\ -\theta_3 & 1 & \theta_1 \\ \theta_2 & -\theta_1 & 1 \end{bmatrix}}^{R^{\mathsf{T}}} \begin{Bmatrix} X_1 \\ X_2 \\ X_3 \end{Bmatrix}$$

correction for orthogonality

$$\begin{Bmatrix} x_1 \\ x_2 \\ x_3 \end{Bmatrix} = \frac{\begin{bmatrix} \theta_1^2\sqrt{1+\theta_1^2+\theta_2^2+\theta_3^2}+\theta_2^2+\theta_3^2 & \theta_3\left(\theta_1^2+\theta_2^2+\theta_3^2\right)+\theta_1\theta_2\left(\sqrt{1+\theta_1^2+\theta_2^2+\theta_3^2}-1\right) & -\theta_2\left(\theta_1^2+\theta_2^2+\theta_3^2\right)+\theta_1\theta_3\left(\sqrt{1+\theta_1^2+\theta_2^2+\theta_3^2}-1\right) \\ -\theta_3\left(\theta_1^2+\theta_2^2+\theta_3^2\right)+\theta_1\theta_2\left(\sqrt{1+\theta_1^2+\theta_2^2+\theta_3^2}-1\right) & \theta_1^2+\theta_2^2\sqrt{1+\theta_1^2+\theta_2^2+\theta_3^2}+\theta_3^2 & \theta_1\left(\theta_1^2+\theta_2^2+\theta_3^2\right)+\theta_2\theta_3\left(\sqrt{1+\theta_1^2+\theta_2^2+\theta_3^2}-1\right) \\ \theta_2\left(\theta_1^2+\theta_2^2+\theta_3^2\right)+\theta_1\theta_3\left(\sqrt{1+\theta_1^2+\theta_2^2+\theta_3^2}-1\right) & -\theta_1\left(\theta_1^2+\theta_2^2+\theta_3^2\right)+\theta_2\theta_3\left(\sqrt{1+\theta_1^2+\theta_2^2+\theta_3^2}-1\right) & \theta_1^2+\theta_2^2+\theta_3^2\sqrt{1+\theta_1^2+\theta_2^2+\theta_3^2} \end{bmatrix}}{\left(\theta_1^2+\theta_2^2+\theta_3^2\right)\sqrt{1+\theta_1^2+\theta_2^2+\theta_3^2}} \begin{Bmatrix} X_1 \\ X_2 \\ X_3 \end{Bmatrix}$$

- In OpenFAST v4, substructure rotation is no longer restricted to limited angles, relying instead on a yaw-pitch-roll sequence:

$$R(\alpha,\beta,\gamma) = R_z(\gamma)R_y(\beta)R_x(\alpha)$$

[3] Jonkman, J.M., (2009). Dynamics of offshore floating wind turbines—model development and verification, *Wind Energy*, **12**(5):459-492. doi:10.1002/we.347.

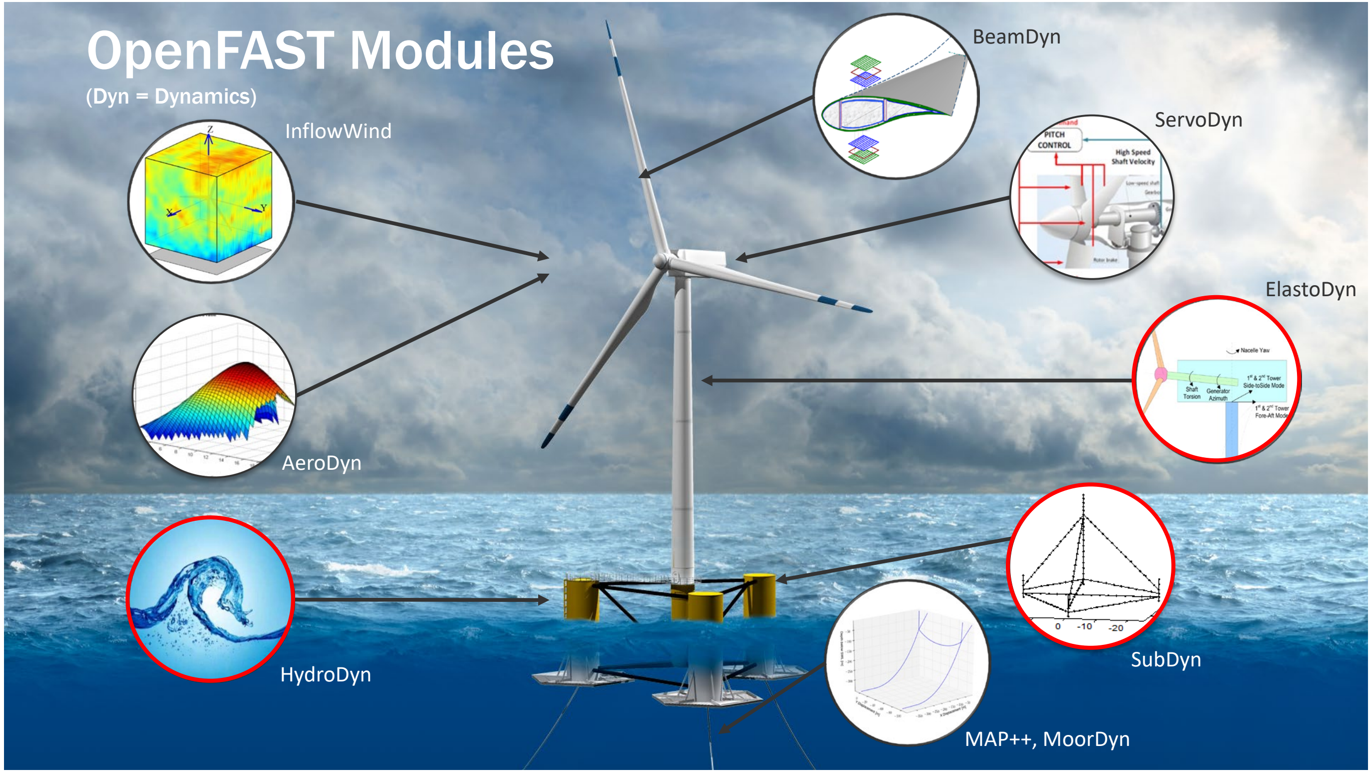

Modules currently relying on small angle platform rotation:

- ElastoDyn: Platform, tower, and wind turbine dynamics
- SubDyn: Substructure/platform elasticity
- HydroDyn: Substructure/platform hydrodynamics

Updates to ElastoDyn

ElastoDyn upgrade to allow arbitrary platform rotation

ElastoDyn uses Kane's method [4] to assemble the equations of motion (EoM) for the system:

$$F_r + F_r^* = 0$$

r is the number of the generalized degree of freedom (DoF). Currently, $r = 1,2,\dots,24$ for a three-bladed rotor, including 6-DoF platform motion, 4 tower-bending DoF, 1 yaw-bearing and 2 drive-train DoF, 2 furling DoF, and 9 blade-bending DoF.

Generalized active forces/moments:

$$F_r = \sum_{i=1}^{w} {}^{E}\boldsymbol{v}_r^{X_i} \cdot \boldsymbol{F}^{X_i} + {}^{E}\boldsymbol{\omega}_r^{N_i} \cdot \boldsymbol{M}^{N_i}$$

Generalized inertia forces/moments:

$$F_r^* = \sum_{i=1}^{w} {}^{E}\boldsymbol{v}_r^{X_i} \cdot \left(-m^{N_i}\,{}^{E}\boldsymbol{a}^{X_i}\right) + {}^{E}\boldsymbol{\omega}_r^{N_i} \cdot \left(-{}^{E}\dot{\boldsymbol{H}}^{N_i}\right)$$

with w rigid bodies labeled N_1 to N_w having center of mass X_i. All equations are solved in the *E*arth-fixed frame.

Notes:

- The **partial (angular) velocities** ${}^{E}\boldsymbol{v}_r^{X_i}$ and ${}^{E}\boldsymbol{\omega}_r^{N_i}$ convert the rigid-body EoM to equations for the generalized DoF.
- This formulation is general and not inherently limited to small rotation, but the current implementation uses small angle rotations for the platform kinematics. This needs to be updated to allow unrestricted platform rotation.
- Tower and blade flexibility are treated via the Rayleigh-Ritz method using mode shapes as shape functions.

[4] Kane, T.R. and Levinson, D.A., (1985). *Dynamics: theory and applications*, New York: McGraw-Hill Book Company.

ElastoDyn upgrade to allow arbitrary platform rotation

Angular velocity of the platform

Small angle formulation: $\,^{E}\boldsymbol{\omega}^{X} = \dot{q}_R \boldsymbol{z}_1 + \dot{q}_Y \boldsymbol{z}_2 - \dot{q}_P \boldsymbol{z}_3 = \sum_{r=4}^{6} \,^{E}\boldsymbol{\omega}_r^{X} \dot{q}_r$

Exact formulation: $\,^{E}\boldsymbol{\omega}^{X} = \dot{q}_R \boldsymbol{\beta}_1 + \dot{q}_Y \boldsymbol{z}_2 - \dot{q}_P \boldsymbol{\alpha}_3 = \sum_{r=4}^{6} \,^{E}\boldsymbol{\omega}_r^{X} \dot{q}_r$

Partial angular velocity of the platform

- Small-angle

$$\,^{E}\boldsymbol{\omega}_r^{X} = \begin{cases} \boldsymbol{z}_1 & \text{for } r = R\ (4) \\ -\boldsymbol{z}_3 & \text{for } r = P\ (5) \\ \boldsymbol{z}_2 & \text{for } r = Y\ (6) \end{cases}$$

- Exact

$$\,^{E}\boldsymbol{\omega}_r^{X} = \begin{cases} \boldsymbol{\beta}_1(t) & \text{for } r = R\ (4) \\ -\boldsymbol{\alpha}_3(t) & \text{for } r = P\ (5) \\ \boldsymbol{z}_2 & \text{for } r = Y\ (6) \end{cases}$$

Nomenclature

E	Earth-fixed/inertial frame
X	Platform orientation
R	Roll angle
P	Pitch angle
Y	Yaw angle
r	Index of DoF. Roll (4), pitch (5), and yaw (6).
q_r	Time-dependent mode “displacement”
$\boldsymbol{z}_i$	Unit vectors along earth-fixed axes.
$\boldsymbol{\alpha}_i$	Unit vectors along body-fixed axes after yaw
$\boldsymbol{\beta}_i$	Unit vectors along body-fixed axes after yaw and pitch

Angular acceleration of the platform

$$\,^{E}\boldsymbol{\alpha}^{X}(\ddot{q}, \dot{q}, q, t) = \left(\sum_r \,^{E}\boldsymbol{\omega}_r^{X}(q,t)\ddot{q}_r\right) + \left[\sum_r \frac{\mathrm{d}}{\mathrm{d}t}\left(\,^{E}\boldsymbol{\omega}_r^{X}(q,t)\right)\dot{q}_r\right]$$

- Small-angle $\frac{\mathrm{d}}{\mathrm{d}t}\left(\,^{E}\boldsymbol{\omega}_r^{X}(q,t)\right) = 0$

- Exact

$$\frac{\mathrm{d}}{\mathrm{d}t}\left(\,^{E}\boldsymbol{\omega}_r^{X}(q,t)\right) = \begin{cases} (\boldsymbol{z}_2 \dot{q}_Y - \boldsymbol{\alpha}_3 \dot{q}_P) \times \,^{E}\boldsymbol{\omega}_r^{X} & \text{for } r = R \\ (\boldsymbol{z}_2 \dot{q}_Y) \times \,^{E}\boldsymbol{\omega}_r^{X} & \text{for } r = P \\ 0 & \text{otherwise} \end{cases}$$

The modifications and additional terms to platform kinematics are “propagated” to the rest of the structure when setting up the EoM.

Updates to SubDyn

SubDyn for floating structures – OpenFAST modular framework for flexible substructures

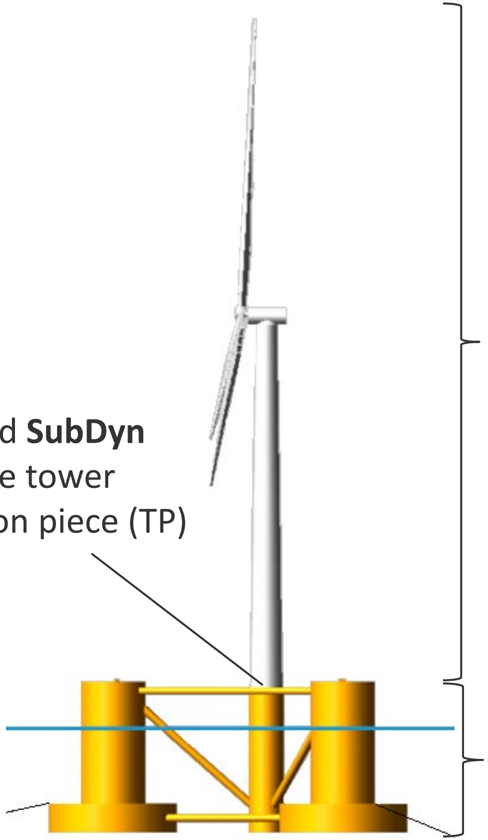

ElastoDyn and **SubDyn** coupled at the tower base/transition piece (TP)

Tower and rotor-nacelle assembly in **ElastoDyn**

Substructure modeled in **SubDyn**

At each time step,

- SubDyn computes the reaction loads from the platform at the tower-base/transition-piece joint as an input to ElastoDyn.
- ElastoDyn computes the motion at the tower-base interface joint as an input to SubDyn.
- the OpenFAST glue-code ensures the ElastoDyn motion and SubDyn reaction load are consistent.

SubDyn for floating structures – Craig-Bampton reduction

- SubDyn is a linear-frame finite-element solver. The EoM for the flexible structure are of the form:

$$\begin{bmatrix} M_{RR} & M_{RL} \\ M_{LR} & M_{LL} \end{bmatrix} \begin{bmatrix} \ddot{U}_R \\ \ddot{U}_L \end{bmatrix} + \begin{bmatrix} C_{RR} & C_{RL} \\ C_{LR} & C_{LL} \end{bmatrix} \begin{bmatrix} \dot{U}_R \\ \dot{U}_L \end{bmatrix} + \begin{bmatrix} K_{RR} & K_{RL} \\ K_{LR} & K_{LL} \end{bmatrix} \begin{bmatrix} U_R \\ U_L \end{bmatrix} = \begin{bmatrix} F_R \\ F_L \end{bmatrix}$$

R Boundary node (e.g., tower base) degrees of freedom

L Interior node degrees of freedom

- SubDyn uses Craig-Bampton reduction [5] to reduce the number of DoF:

$$\begin{bmatrix} U_R \\ U_L \end{bmatrix} = \begin{bmatrix} I & 0 \\ \Phi_R & \Phi_m \end{bmatrix} \begin{bmatrix} U_R \\ q_m \end{bmatrix}$$

q_m are the amplitudes of a truncated set of Craig-Bampton internal elastic modes with

$$\mathrm{size}(q_m) \ll \mathrm{size}(U_L)$$

- The equations of motion can be reformulated to

0 if floating

$$\begin{bmatrix} M_{BB} & M_{Bm} \\ M_{mB} & I \end{bmatrix} \begin{bmatrix} \ddot{U}_{TP} \\ \ddot{q}_m \end{bmatrix} + \begin{bmatrix} C_{BB} & 0 \\ 0 & C_{mm} \end{bmatrix} \begin{bmatrix} \dot{U}_{TP} \\ \dot{q}_m \end{bmatrix} + \begin{bmatrix} \cancel{K_{BB}} & 0 \\ 0 & K_{mm} \end{bmatrix} \begin{bmatrix} U_{TP} \\ q_m \end{bmatrix} = \begin{bmatrix} F_{TP} \\ F_m \end{bmatrix}$$

U_{TP} is the Guyan mode displacement, i.e., the displacement of the transition piece to which all boundary nodes are rigidly attached.

[5] Craig Jr., R.R. and Bampton, M.C.C., (1968). Coupling of substructure for dynamic analysis, *AIAA J.*, **6**(7):1313-1319. doi:10.2514/3.4741.

SubDyn for floating structures – Existing correction for floating structures

- SubDyn takes U_{TP} from ElastoDyn as input and returns the reaction load at TP:

$$\begin{bmatrix} M_{BB} & M_{Bm} \\ M_{mB} & I \end{bmatrix}\begin{bmatrix} \ddot{U}_{TP} \\ \ddot{q}_m \end{bmatrix} + \begin{bmatrix} C_{BB} & 0 \\ 0 & C_{mm} \end{bmatrix}\begin{bmatrix} \dot{U}_{TP} \\ \dot{q}_m \end{bmatrix} + \begin{bmatrix} 0 & 0 \\ 0 & K_{mm} \end{bmatrix}\begin{bmatrix} U_{TP} \\ q_m \end{bmatrix} = \begin{bmatrix} F_{TP} \\ F_m \end{bmatrix}$$

Re-arranging gives the following expression for the reaction load:

$$\begin{aligned} -F_{TP,React} = & \boxed{\begin{aligned} &-[M_{Bm}K_{mm}]q_m - [M_{Bm}C_{mm}]\dot{q}_m \\ &-[M_{Bm}M_{mB}]\ddot{U}_{TP} + [M_{Bm}\Phi_m^T]F_L \end{aligned}} && \text{(Inertial contribution from elastic deformation, } \ddot{q}_m\text{)} \\ & +[C_{BB}]\dot{U}_{TP} + [M_{BB}]\ddot{U}_{TP} && \text{(Contribution from rigid-body motion)} \\ & -[T_I^T\Phi_R^T]F_L - [T_I^T]F_R && \text{(Direct contribution from external loads)} \end{aligned}$$

- Existing floating correction implementation:

The EoM for $\ddot{q}_m$ are interpreted to be in a frame of reference following the Guyan mode (rigid-body motion), so elastic deformation is small:

$$\begin{aligned} -F_{TP,React} = & -[R_{b2g}M_{Bm}K_{mm}]q_m - [R_{b2g}M_{Bm}C_{mm}]\dot{q}_m \\ & -[R_{b2g}M_{Bm}M_{mB}R_{g2b}]\ddot{U}_{TP} + [R_{b2g}M_{Bm}\Phi_m^T R_{g2b}]F_L && \text{(Contribution from } \ddot{q}_m\text{)} \\ & +[C_{BB}]\dot{U}_{TP} + [M_{BB}]\ddot{U}_{TP} && \text{(Contribution from rigid-body motion)} \\ & -[T_I^T\Phi_R^T]F_L - [T_I^T]F_R && \text{(Direct contribution from external loads)} \end{aligned}$$

The rigid-body motion part is still linearized and only works for small platform rotation.

- SubDyn takes U_{TP} from ElastoDyn as input and returns the reaction load at TP:

$$\begin{bmatrix} M_{BB} & M_{Bm} \\ M_{mB} & I \end{bmatrix} \begin{bmatrix} \ddot{U}_{TP} \\ \ddot{q}_m \end{bmatrix} + \begin{bmatrix} C_{BB} & 0 \\ 0 & C_{mm} \end{bmatrix} \begin{bmatrix} \dot{U}_{TP} \\ \dot{q}_m \end{bmatrix} + \begin{bmatrix} 0 & 0 \\ 0 & K_{mm} \end{bmatrix} \begin{bmatrix} U_{TP} \\ q_m \end{bmatrix} = \begin{bmatrix} F_{TP} \\ F_m \end{bmatrix}$$

Re-arranging gives the following expression for the reaction load:

$$\begin{aligned} -F_{TP,React} = & \boxed{\begin{aligned} &-[M_{Bm}K_{mm}]q_m - [M_{Bm}C_{mm}]\dot{q}_m \\ &-[M_{Bm}M_{mB}]\ddot{U}_{TP} + [M_{Bm}\Phi_m^T]F_L \end{aligned}} && \text{(Inertial contribution from elastic deformation, } \ddot{q}_m\text{)} \\ & +[C_{BB}]\dot{U}_{TP} + [M_{BB}]\ddot{U}_{TP} && \text{(Contribution from rigid-body motion)} \\ & -[T_I^T\Phi_R^T]F_L - [T_I^T]F_R && \text{(Direct contribution from external loads)} \end{aligned}$$

- Updated floating correction for unrestricted rigid-body motion and small elastic deformation:

$$\begin{aligned} -F_{TP,React} = & -[R_{b2g}M_{Bm}K_{mm}]q_m - [R_{b2g}M_{Bm}C_{mm}]\dot{q}_m \\ & -[R_{b2g}M_{Bm}M_{mB}R_{g2b}]\begin{bmatrix} \dot{V}_{TP} \\ \dot{\omega}_{TP} \end{bmatrix} + [R_{b2g}M_{Bm}\Phi_m^T R_{g2b}]F_L && \text{(From } \ddot{q}_m\text{)} \\ & +[R_{b2g}C_{BB}R_{g2b}]\begin{bmatrix} V_{TP} \\ \omega_{TP} \end{bmatrix} + [R_{b2g}M_{BB}R_{g2b}]\begin{bmatrix} \dot{V}_{TP} \\ \dot{\omega}_{TP} \end{bmatrix} + \begin{bmatrix} m_{BB}\omega_{TP} \times (\omega_{TP} \times [R_{b2g}]r_{PG}) \\ \omega_{TP} \times [R_{b2g}I_{BB}R_{g2b}]\omega_{TP} \end{bmatrix} && \text{(Rigid-body part)} \\ & -[R_{b2g}T_I^T\Phi_R^T R_{g2b}]F_L - [R_{b2g}T_I^T R_{g2b}]F_R && \text{(External loads)} \end{aligned}$$

While the elastic deformation is still based on linear superposition (in a frame following rigid-body motion), the rigid-body motion is now nonlinear and exact for large rotation.

Updates to HydroDyn

Extensions to HydroDyn potential-flow models – Linear wave excitation

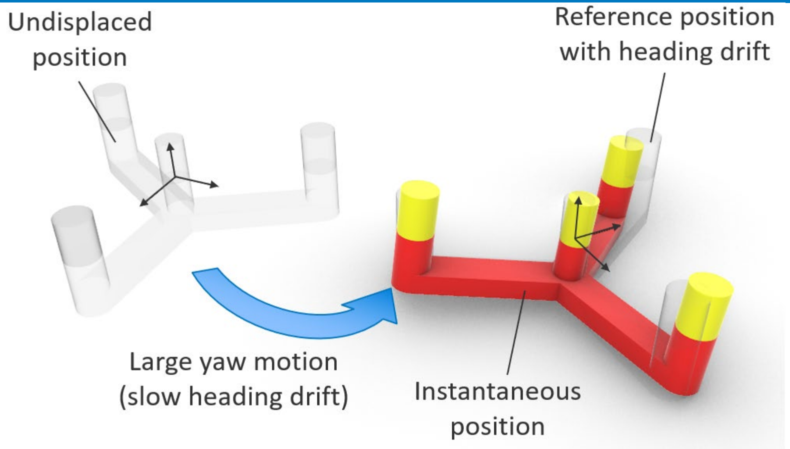

Platform Rotation matrix with two contributions to yaw ($\gamma = \bar{\gamma} + \gamma'$):

$$R = R_z(\gamma)R_y(\beta)R_x(\alpha)$$
$$= \underbrace{R_z(\bar{\gamma})}_{\text{Large/slow heading change}} \quad \underbrace{R_z(\gamma')R_y(\beta)R_x(\alpha)}_{R' \text{ (small rotation)}}$$

Slow heading change based on low-pass filtered yaw angle:

$$\bar{\gamma}^n = C\bar{\gamma}^{n-1} + (1-C)\gamma^n$$
$$C = \exp(-2\pi\Delta t f_{cutoff})$$

α	Roll angle
β	Pitch angle
γ	Yaw angle

Wave-grid introduced in OpenFAST 4.0 [6]

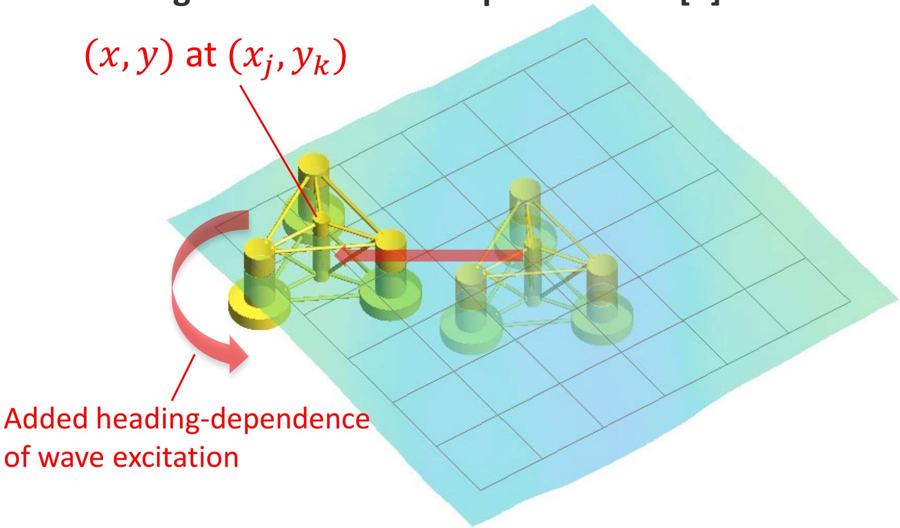

Linear potential-flow wave excitation is precomputed with the structure located at each grid point (x_j, y_k) and for an array of possible headings, γ_l:

$$F^{(1)}_{ex,m,h}(t; x_j, y_k, \gamma_l)$$
$$= \Re\left\{\sum_{n=1}^{N} A_n(x_j, y_k) X^{(1)}_m(\omega_n, \beta_n - \gamma_l) e^{i\omega_n t}\right\}$$

The instantaneous wave excitation is interpolated based on t, x, y, and $\bar{\gamma}$ from $F^{(1)}_{ex,m}(t; x_j, y_k, \gamma_l)$.

[6] Wang, L., Jonkman, J., Hayman, G., Platt, A., Jonkman, B., and Robertson, A., (2022). Recent hydrodynamic modeling enhancements in OpenFAST, in Proc. ASME 4th Int. Offshore Wind Tech. Conf., Boston, MA, USA. doi:10.1115/IOWTC2022-98094.

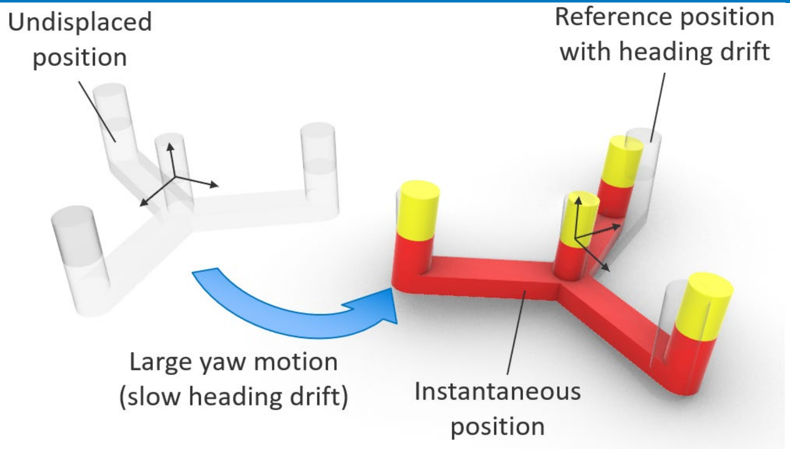

Platform Rotation matrix with two contributions to yaw ($\gamma = \bar{\gamma} + \gamma'$):

$$R = R_z(\gamma)R_y(\beta)R_x(\alpha)$$
$$= \underbrace{R_z(\bar{\gamma})}_{\substack{\text{Large/slow}\\ \text{heading change}}} \quad \underbrace{R_z(\gamma')R_y(\beta)R_x(\alpha)}_{R' \text{ (small rotation)}}$$

Slow heading change based on low-pass filtered yaw angle:

$$\bar{\gamma}^n = C\bar{\gamma}^{n-1} + (1-C)\gamma^n$$
$$C = \exp(-2\pi\Delta t f_{cutoff})$$

α	Roll angle
β	Pitch angle
γ	Yaw angle

Second-order mean-drift and slow-drift (Newman's approximation) are similarly precomputed for all wave headings and interpolated during simulation.

Second-order mean drift load

$$F_{d,m,h}^{(2)}(\gamma_l) = \sum_{n=1}^{N} \left|A_{n,0}\right|^2 X_{d,m}^{(2)}(\omega_n, \beta_n - \gamma_l)$$

Second-order slow-drift load with Newman's approximation [7]

$F_{ex,m,h}^{(2-)}(t; x_j, y_k, \gamma_l)$ (x and y dependence not implemented)

$$= \left|\sum_{n=1}^{N} A_n(x_j, y_k)\sqrt{X_{d,m}^{(2)}(\omega_n, \beta - \gamma_l)}e^{i\omega_n t}\right|^2_{X_{d.m}^{(2)}(\omega_n,\beta-\gamma_l)>0} - \left|\sum_{n=1}^{N} A_n(x_j, y_k)\sqrt{-X_{d,m}^{(2)}(\omega_n, \beta - \gamma_l)}e^{i\omega_n t}\right|^2_{X_{d.m}^{(2)}(\omega_n,\beta-\gamma_l)<0}$$

Note that we currently do not support dynamic large yaw offset with full sum- and difference-frequency QTFs.

[7] Standing, R.G., Brending, W.J., and Wilson, D., (1987). Recent developments in the analysis of wave drift forces, low-frequency damping and response, in *Proc. Offshore Tech. Conf.*, Houston, TX, USA. doi:10.4043/5456-MS.

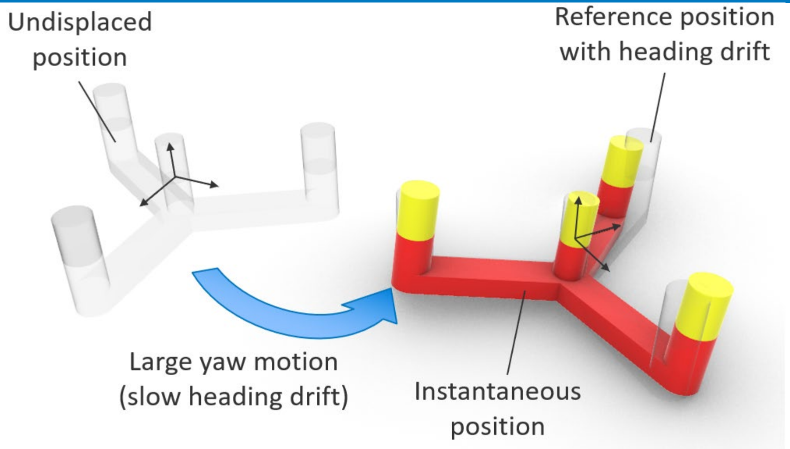

Platform Rotation matrix with two contributions to yaw ($\gamma = \bar{\gamma} + \gamma'$):

$$R = R_z(\gamma)R_y(\beta)R_x(\alpha)$$
$$= \underbrace{R_z(\bar{\gamma})}_{\substack{\text{Large/slow}\\ \text{heading change}}} \underbrace{R_z(\gamma')R_y(\beta)R_x(\alpha)}_{R'\ (\text{small rotation})}$$

Slow heading change based on low-pass filtered yaw angle:

$$\bar{\gamma}^n = C\bar{\gamma}^{n-1} + (1-C)\gamma^n$$
$$C = \exp(-2\pi\Delta t f_{cutoff})$$

α	Roll angle
β	Pitch angle
γ	Yaw angle

Wave-radiation loads based on Cummins equation [8]:

$$F_{i,h}^{Rad}(t) = -A_{ij}^{\infty} a_{h,j}(t) - \int_0^t K_{ij}(t-\tau)v_{h,j}(\tau)\mathrm{d}\tau$$

- Platform acceleration and velocity $\boldsymbol{a}_h$ and $\boldsymbol{v}_h$ are resolved in the h(eading) frame yawed from the earth-fixed frame by $\bar{\gamma}$.
- The forces and moments are transformed back to the earth-fixed frame.
- Similar approach adopted for the state-space model.

Hydrostatic loads

$$F_{i,Y}^{Hst}(t) = \sum_{j=3}^{5} C_{ij}q_j(t) + F_{i,0}^{Hst}$$

- Platform displacement and hydrostatic force computed in the Y(aw) frame yawed from the earth-fixed frame by $\gamma(t)$. Exact pitch/roll rotations are used for consistency with updated ElastoDyn, but these angles must be small.
- Any roll-yaw and pitch-yaw coupling in the stiffness matrix, C_{ij}, due to center of buoyancy offset are included when transforming the constant hydrostatic load for an undisplaced platform, $F_{i,0}^{Hst}$, back to the earth-fixed frame.

[8] Cummins, W.E., (1962). The impulse response function and ship motions, *Schiffstechnik* **9**:101-109.

Example simulation with the loss of a mooring line

Example with large platform yaw motion following the loss of a mooring line

An example with mooring-line failure

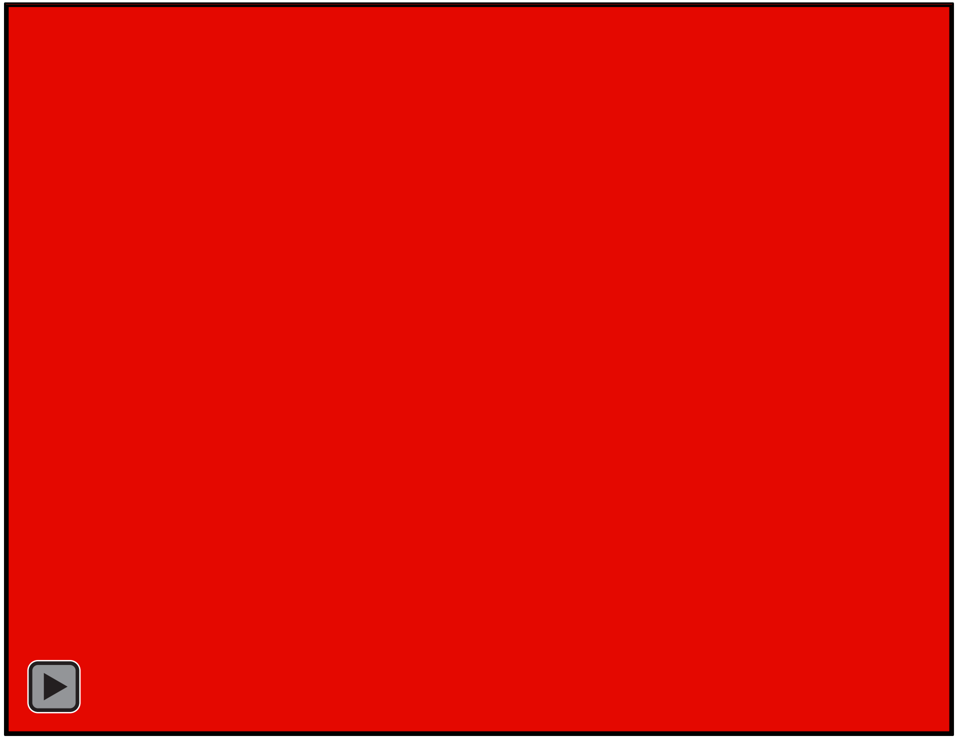

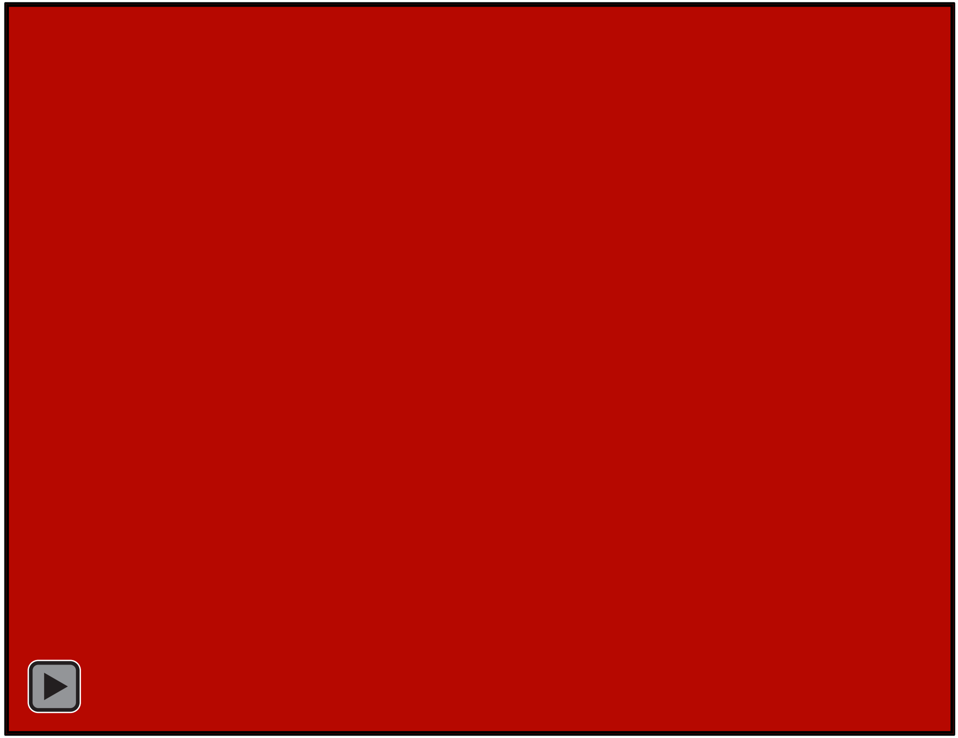

Example with large platform yaw motion following the loss of a mooring line

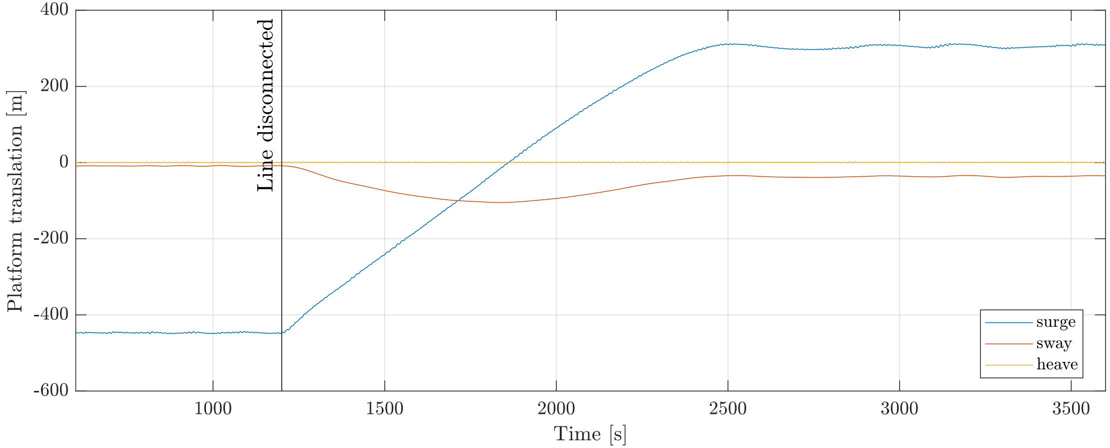

Time series of platform translation

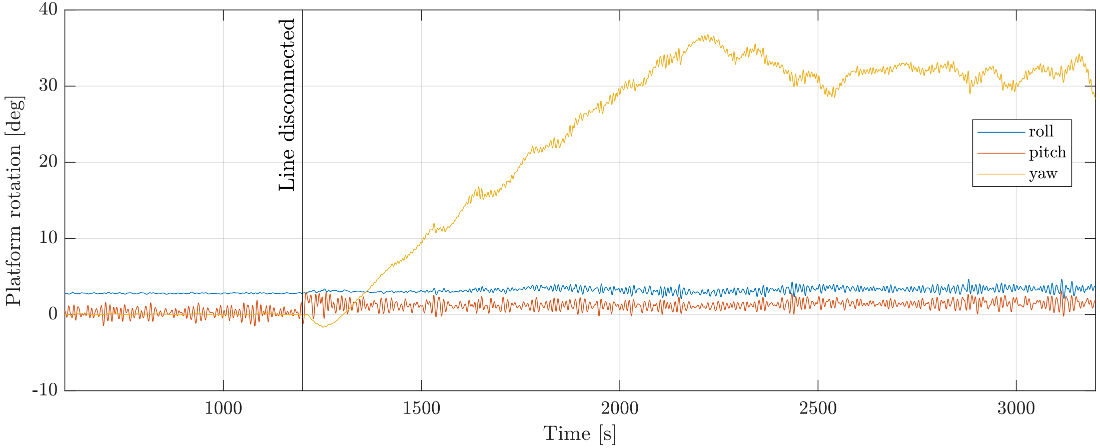

Time series of platform rotation

- Example of a coupled aero-hydro-servo-elastic simulation with the loss of a mooring line and large platform translation and rotation.
- OpenFAST now accommodates both large translation and rotation (yaw up to 35 deg in this example).

Example with large platform yaw motion following the loss of a mooring line

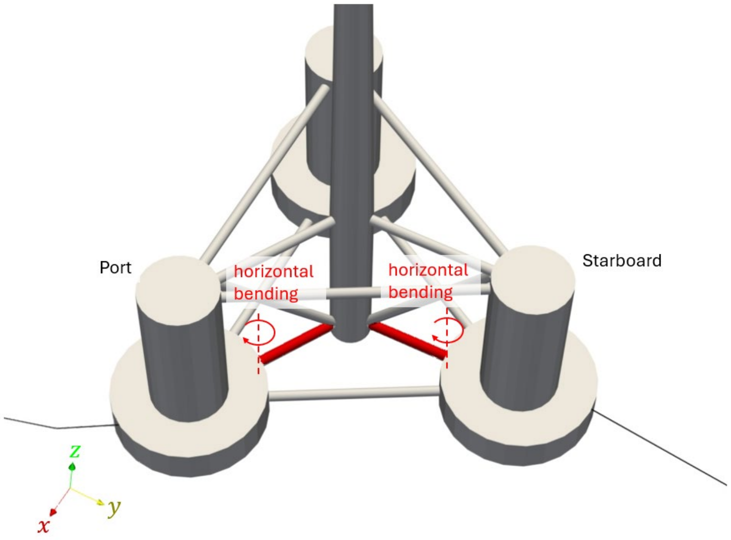

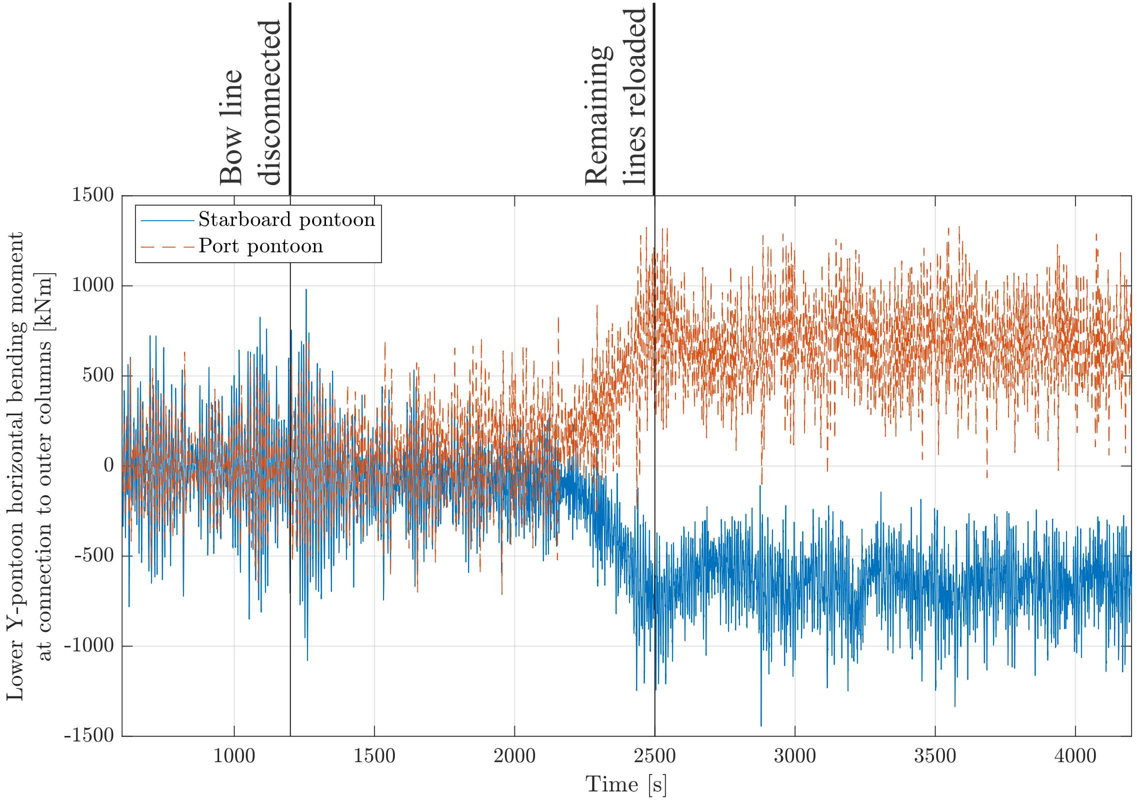

Horizontal-plane bending moment in the aft lower Y-pontoons

Thank You

www.nrel.gov

This work was authored by the National Renewable Energy Laboratory, operated by Alliance for Sustainable Energy, LLC, for the U.S. Department of Energy (DOE) under Contract No. DE-AC36-08GO28308. Funding provided by the U.S. Department of Energy Advanced Research Projects Agency-Energy (ARPA-E) under the project titled "Wind Energy with Integrated Servo-control (WEIS): A Toolset to Enable Controls Co-Design of Floating Offshore Wind Energy (Phase 2)." The views expressed in the article do not necessarily represent the views of the DOE or the U.S. Government. The U.S. Government retains and the publisher, by accepting the article for publication, acknowledges that the U.S. Government retains a nonexclusive, paid-up, irrevocable, worldwide license to publish or reproduce the published form of this work, or allow others to do so, for U.S. Government purposes.

Photo from iStock-627281636

NREL

Transforming ENERGY